Developmental Biology 380 (2013) 314–323

Contents lists available at SciVerse ScienceDirect

Developmental Biology

journal homepage: www.elsevier.com/locate/developmentalbiology

The LIM homeobox gene *ceh-14* is required for phasmid function and neurite outgrowth

Hiroshi Kagoshima [a,b,c], Giuseppe Cassata [a,1], Yong Guang Tong [d,e,2], Nathalie Pujol [f,g,h], Gisela Niklaus [a,3], Thomas R. Bürglin [a,d,e,*]

[a] Biozentrum, Universität Basel, Klingelbergstrasse 70, CH-4056 Basel, Switzerland
[b] Genome Biology Laboratory, Center for Genetic Resource Information, National Institute of Genetics, Yata 1111, Mishima, Shizuoka 411-8540, Japan
[c] Transdisciplinary Research Integration Center, Research Organization of Information and Systems (ROIS), Toranomon 4-3-13, Minato-ku, Tokyo 105-0001, Japan
[d] Department of Biosciences and Nutrition, Karolinska Institutet, Hälsovägen 7, Novum, SE-141 83 Huddinge, Sweden
[e] School of Life Sciences, Södertörn University, Alfred Nobels Allé 7, SE-141 89 Huddinge, Sweden
[f] Centre d'Immunologie de Marseille-Luminy, UM2 Aix-Marseille Université, Case 906, 13288 Marseille CEDEX 09, France
[g] INSERM, U1104, 13288 Marseille, France
[h] CNRS, UMR7280, 13288 Marseille, France

ARTICLE INFO

Article history:
Received 11 February 2013
Received in revised form
29 March 2013
Accepted 4 April 2013
Available online 19 April 2013

Keywords:
Homeobox gene
LIM domain
ceh-14
Caenorhabditis elegans
Neurite outgrowth
Neural development
Phasmids

ABSTRACT

Transcription factors play key roles in cell fate specification and cell differentiation. Previously, we showed that the LIM homeodomain factor CEH-14 is expressed in the AFD neurons where it is required for thermotaxis behavior in *Caenorhabditis elegans*. Here, we show that *ceh-14* is expressed in the phasmid sensory neurons, PHA and PHB, a number of neurons in the tail, i.e., PHC, DVC, PVC, PVN, PVQ, PVT, PVW and PVR, as well as the touch neurons. Analysis of the promoter region shows that important regulatory elements for the expression in most neurons reside from −4 kb to −1.65 kb upstream of the start codon. Further, within the first introns are elements for expression in the hypodermis. Phylogenetic footprinting revealed numerous conserved motifs in these regions. In addition to the existing deletion mutation *ceh-14*(*ch3*), we isolated a new allele, *ceh-14*(*ch2*), in which only one LIM domain is disrupted. The latter mutant allele is partially defective for thermosensation. Analysis of both mutant alleles showed that they are defective in phasmid dye-filling. However, the cell body, dendritic outgrowth and ciliated endings of PHA and PHB appear normal, indicating that *ceh-14* is not required for growth. The loss of a LIM domain in the *ceh-14*(*ch2*) allele causes a partial loss-of-function phenotype. Examination of the neurites of ALA and tail neurons using a *ceh-14*::*GFP* reporter shows abnormal axonal outgrowth and pathfinding.

© 2013 Elsevier Inc. All rights reserved.

Introduction

The homeodomain is an evolutionary conserved DNA-binding domain found in many eukaryotes ranging from plants to human (for review see Bürglin, 2011). The LIM homeobox (LIM-HB) genes are one class of many different types of homeobox genes and characteristically contain two LIM domains amino-terminal to the homeodomain (Hobert and Westphal, 2000; Srivastava et al., 2010). The LIM domain was named after the first three founding genes, *lin-11*, *islet-1* and *mec-3* (Freyd et al., 1990; Karlsson et al., 1990; Way and Chalfie, 1988). It consists of two zinc-finger-like motifs with a highly conserved pattern of cysteine and histidine residues, which mediate protein–protein interactions (for review see Dawid et al., 1998; Kadrmas and Beckerle, 2004; Koch et al., 2012; Zheng and Zhao, 2007).

LIM homeodomain (LIM-HD) proteins play pivotal roles in cell fate determination and differentiation in a variety of developmental processes. In particular, their function is critical in different aspects of neuronal development, including neuronal specification, neuronal survival, and neurotransmitter expression (e.g., Hobert and Westphal, 2000; Lundgren et al., 1995; Pfaff et al., 1996; Thaler et al., 2004; Way and Chalfie, 1988), as well as axonal outgrowth and pathfinding (e.g., Kania et al., 2000; Sharma et al., 2000; Thor et al., 1999). In flies and vertebrates, it has been shown that the cell type-specific combinatorial expression of LIM-HD factors defines the identities of subclasses of motor neurons, i.e. the specific pattern of axonal outgrowth and the targets of

* Corresponding author at: Department of Biosciences and Nutrition, Karolinska Institutet, Hälsovägen 7, Novum, SE-141 83 Huddinge, Sweden, Fax: +46 8 524 81130.
E-mail address: thomas.burglin@ki.se (T.R. Bürglin).
[1] Present address: Roche Pharma (Schweiz) AG, Schönmattstrasse 2, 4153 Reinach, Switzerland.
[2] Present address: National Institute of Environmental Health Sciences, 111 T.W. Alexander Drive, MD E1-05, Research Triangle Park, NC 27709, USA.
[3] Present address: Geistlich Pharma AG, Zellbiologie, 6110 Wolhusen, Switzerland.

0012-1606/$ - see front matter © 2013 Elsevier Inc. All rights reserved.
http://dx.doi.org/10.1016/j.ydbio.2013.04.009

their projection (O'Keefe et al., 1998; Sharma et al., 1998; Thor et al., 1999). In *C. elegans*, mutations in the LIM-HB genes *ttx-3*, *lin-11* and *lim-6* cause axonal defects (Hobert et al., 1998, 1997, 1999). Other classes of homeobox genes have been shown to play roles in these processes as well (Landgraf et al., 1999; Thaler et al., 1999), and in *C. elegans*, for example, the paired-like homeobox gene *ceh-17* is involved in outgrowth of the ALA axons (Pujol et al., 2000; Van Buskirk and Sternberg, 2010).

A series of experiments in which the LIM domain was truncated or mutated suggested that it might act as an intramolecular negative regulatory element by inhibiting the DNA binding activity of the homeodomain (Sánchez-García et al., 1993). Thus, such LIM-disrupted LIM-HB genes would encode gain-of-function forms of LIM-HD transcription factors (Agulnick et al., 1996). However, the disruption of the LIM domain of the LIM-HB genes *apterous* and *lim3* showed phenotypes similar to the null mutations of the corresponding genes in *Drosophila* (O'Keefe et al., 1998; Thor et al., 1999). These results suggest that the LIM domain is also required for the function and LIM-disruption mutations result in loss-of-function mutations.

We previously described the role of *ceh-14* in thermosensation in *C. elegans* (Cassata et al., 2000a). *ceh-14* belongs to the LIM3 (Lhx3/Lhx4) family of LIM-HB genes and is orthologous to fly Lim3 and vertebrate Lhx3 and Lhx4 (Bürglin, 2011; Hobert and Westphal, 2000). In the present paper, we examine the expression pattern of *ceh-14* in the nervous system and other tissues using a series of deletion reporter constructs. We find that *ceh-14* is involved in neurite outgrowth in subsets of neurons and essential for the proper function of the phasmid sensory neurons. We also present data for a *ceh-14*(*ch2*) mutation allele, in which a LIM domain has been deleted, and which causes partial loss-of-function phenotypes.

Materials and methods

Reporter constructs

General DNA manipulations were carried out as described (Ausubel et al., 1987; Sambrook and Russell, 2001). pLZ14-2 is a lacZ reporter construct (Fire et al., 1990), containing 4.8 kb of upstream sequence together with the coding sequence up to the splice acceptor of the fifth exon of *ceh-14*. pHK103 and pHK107 are green fluorescent protein (GFP) reporters, containing 4.0 kb of upstream sequence and the first 16 amino acids of CEH-14, with or without a SV40 nuclear localization signal (NLS). pHK106 and pHK108 contain 4.0 kb of upstream sequence and the entire coding sequence of *ceh-14* fused to GFP, with or without NLS. GFP reporter constructs were made by a two-step long-range PCR method (Cassata et al., 1998). pHK160 has the same sequences as pHK103, except that it contains a GFP-lacZ double reporter. Reporter constructs for promoter analysis (pHK162–pHK167) were made by restriction enzyme digestion and ligation from pHK103, pHK160 and pLZ14-2.

Constructs are referred to here based on the genomic sequence coordinates, which are numbered with respect to the ATG. In brackets the plasmid names are given, some of which are also used in previous publications. In square brackets the sequence coordinates are given based on cosmid F46C8 (accession # U41624); the ATG start codon is from −23320 to −23318, the stop codon is from −19206 to −19204. List of reporter constructs:

p4770E5::lacZ (pLZ14-2): −4771 to 2727 [−28091 to −20593], 4.77 kb promoter, ends at exon 5.
p4000full::GFP (pHK106): −4011 to 4113 [−27331 to −19207], 4 kb promoter, full length *ceh-14*.
p4000full::ΔNGFP (pHK108): −4011 to 4113 [−27331 to −19207], like p4000full::GFP, but no NLS.
p4000E1::GFP (pHK103): −4011 to 47 [−27331 to −23273], 4 kb promoter, ends in exon 1.
p4000E1::ΔNGFP (pHK107): −4011 to 47 [−27331 to −23273], like p4000E1::GFP, but no NLS.
p4000E1::GFPlacZ (pHK160): −4011 to 47 [−27331 to −23273], like p4000E1::GFP, plus lacZ.
p1650E1::GFP (pHK162): −1654 to 47 [−24974 to −23273], 1.65 kb promoter, ends in exon 1.
p1240E1::GFP (pHK163): −1242 to 47 [−24562 to −23273], 1.24 kb promoter, ends in exon 1.
p240E1::GFP (pHK164): −237 to 47 [−23557 to −23273], 240 bp promoter, ends in exon 1.
p240E1::GFPlacZ (pHK167): −237 to 47 [−23557 to −23273], like p240E1::GFP, plus lacZ.
p240E5::lacZ (pHK166): −237 to 2727 [−23557 to −20593], 240bp promoter to exon 5.

Ectopic expression constructs: full length *ceh-14* cDNA was amplified by PCR using p14-31_for (GGCTCCATGGATCCTATGCTGG-GACACAACATTTTG, contains an NcoI site) and p14-32_rev GTCAC-CATGGTAATGTACTGTGGAGTCATGTGTG, contains an NcoI site) and cloned via the NcoI site into prabGFPim3′ (generous gift by M. Nonet, http://thalamus.wustl.edu/nonetlab/ResourcesF/seqinfo.html). The *ceh-14* LIM domain only region was amplified with primers Ceh14lim_for (ACGTACCGGTGATGCTGGGACACAACATTTT, containing an AgeI site) and Ceh14lim_rev (AGCACCATGGGTT-CATTGCAGTGTTTATCTC, containing an NcoI site), and cloned into prabGFPim3′ using AgeI and NcoI.

ceh-14 genomic deletion derivatives

Details of two *ceh-14* deletion alleles, *ceh-14*(*ch1*) and *ceh-14* (*ch3*), are described previously (Cassata et al., 2000a). The third allele, *ceh-14*(*ch2*), was isolated in the same fashion. The deletion in each allele lacks the following sequences: *ceh-14*(*ch1*): −21721 to −20937, *ceh-14*(*ch2*): −21966 to −20938, *ceh-14*(*ch3*): −21980 to −20704 (Cosmid F46C8 numbering). The *ceh-14*(*ch2*) deletion lies between the second intron and the third intron. At the deletion point, an additional seven nucleotides (5′-GTTGTGT-3′) are inserted. The resulting transcript lacks the third exon, but the second exon can splice in frame to the fourth exon.

Worm strains

C. elegans strains were maintained by standard methods (Epstein and Shakes, 1995; Hope, 1999; Wood, 1988). The *C. elegans* strains used in this study were: Bristol strain (N2), MT2709 [*rol-6* (*n1270e187*)*II*], CB1372 [*daf-7*(*e1372*)*III*], CB3775 [*dpy-20*(*e2017*)*IV*], YK11 [*mut-2* (*r459*)*I*; *dpy-19* (*n1347*)*III*; *ceh-14* (*ms11::Tc1*)*X*], TB527 [*ceh-14*(*ch2*)*X*], TB528 [*ceh-14*(*ch3*)*X*], TB521 [*ceh-14*(*ch2*)*X; dpy-20* (*e2017*)*IV*], TB522 [*ceh-14*(*ch3*)*X; dpy-20*(*e2017*)*IV*], TB513 [*chIs513* (*pHK106, pMH86*)*V; dpy-20*(*e2017*)*IV*], TB534 [*chIs513*(*pHK106, pMH86*)*V; dpy-20*(*e2017*)*IV; ceh-14*(*ch2*)*X*], and TB535 [*chIs513* (*pHK106, pMH86*)*V; dpy-20*(*e2017*)*IV; ceh-14*(*ch3*)*X*], and IB16 [*ceh-17*(*np1*)*I*] (Pujol et al., 2000).

Germline transformation

Germline transformation was performed by coinjecting reporter DNA at a concentration of 30–100 μg/ml and marker DNA at a concentration of 5–20 μg/ml into the gonad of animals (Mello et al., 1991). Three transgenic markers were; plasmid pRF4 containing *rol-6* (*su1006*) for selecting rolling phenotype, cosmid DE9 containing *daf-7* (+) for rescuing the dauer constitutive defect of *daf-7*(*e1372*) at 25 °C

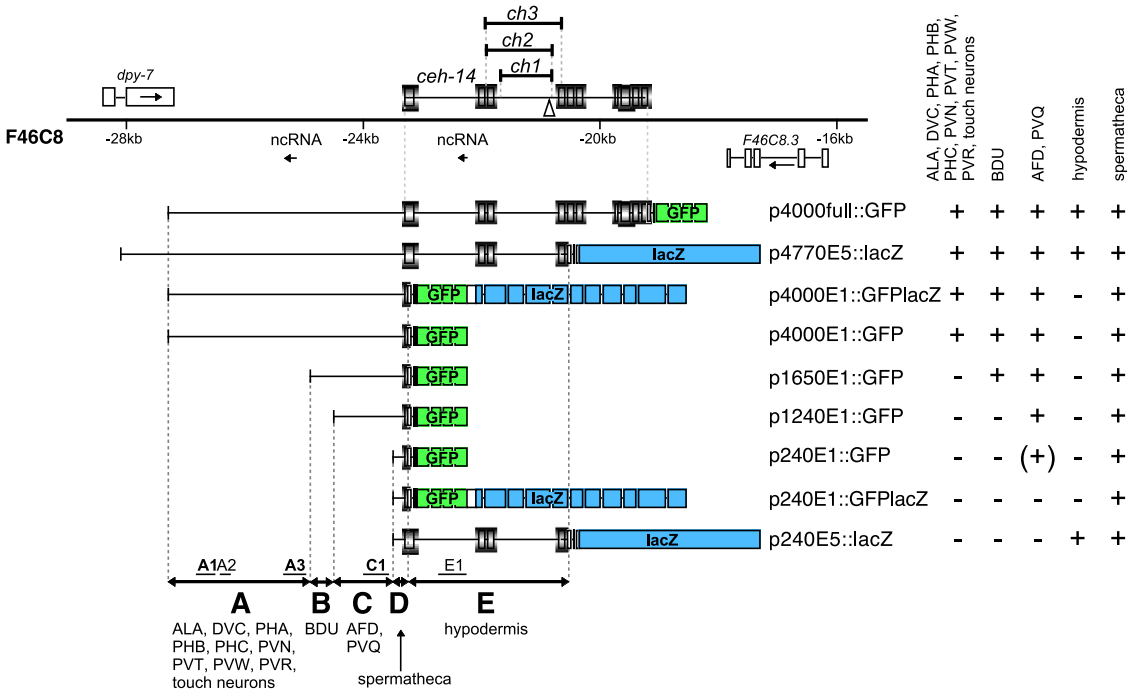

Fig. 1. Structure of the *ceh-14* gene, of the reporter constructs and summary of the expression pattern. Underneath the genomic structure of *ceh-14* on cosmid F46C8 are schematic representations of the reporter constructs used to analyze the expression pattern. Different types of boxes represent coding sequences as follows: gradient boxes: *ceh-14* exons; black boxes: SV40 NLS; green boxes: GFP; blue boxes: lacZ. The table at the right summarizes expression in different cell types (using either + or −). Above the genomic structure, lines indicate the regions which are deleted in the alleles (*ch1*), (*ch2*), and (*ch3*). In the allele *ceh-14*(*ch2*) the third exon is removed, resulting in a protein that lacks most of the first LIM domain. The white triangle indicates the insertion point of the transposon Tc1. At the bottom the different sections of the regulatory region (A–E) are indicated, and subsections (A1–A3, C1, E1) show regions well conserved to *C. briggsae* and *C. remanei* (Supplementary Fig. 1). A1, A3, C1 (in bold) contain putative autoregulatory binding sites for CEH-14 by ChIP-seq (Niu et al., 2011).

and plasmid pMH86 containing *dpy-20*(+) for rescuing *dpy-20*(*e2017*) (Han and Sternberg, 1991). Multiple independent lines were established for each construct. p*rab-3*::*CEH14::GFP* and p*rab-3*::*CEH14-LIM-only::GFP* was injected at 70 μg/ml and coinjected with the marker *elt-2*::*mCherry* at 45 μg/ml.

Staining of worms

LacZ staining: worms were washed off the plates in water, centrifuged several times and resuspended in water, frozen at −70 °C, and freeze-dried in a lyophilizer. They were fixed in acetone and stained at 37 °C for 2 h to overnight with staining solution: 200 mM Na Phosphate pH 7.5, 5 mM K Ferricyanide, 5 mM K Ferrocyanide, 1 mM $MgCl_2$, 0.4% SDS, 0.08% X-gal (Fire, 1992).

DiI (1,1′-dioctadecyl-3,3,3′,3′-tetramethylindocarbocyanine perchlorate, Promega) staining was performed in the same way as FITC staining (Hedgecock et al., 1985), substituting DiI at 10 μg/ml. Stained worms were viewed by fluorescence microscopy using a rhodamine filter.

CEH-17 antibody staining was conducted as previously described (Pujol et al., 2000), and 100 animals were examined.

Behavioral analyses

Single worm thermotaxis assays were performed as previously described (Cassata et al., 2000a; Hedgecock and Russell, 1975; Mori and Ohshima, 1995). The classification of the phenotypes was performed following the criteria shown in (Cassata et al., 2000a). Animals that did not move were not taken into account. Touch sensitivity assays of worms were performed as described (Chalfie and Sulston, 1981).

Measurement of body sizes

Embryos were collected by sodium-hypochlorite treatment of adult animals as described by Lewis and Fleming (Epstein and Shakes, 1995), and incubated in S-basal buffer for 24 h at 25 °C to synchronize at L1 stage. L1 larvae were allowed to develop on NGM plates at 20 °C. The photographs of animals, at 0 h, 24 h, 48 h, and 72 h after L1-arrest release were taken with an Axioplan 2 microscope (Carl Zeiss) and analyzed with AQUACOSMOS (Hamamatsu Photonics). The length (l) and the area of the longitudinal section (s) of animals were measured with ImageJ (http://rsb.info.nih.gov/ij/) using a Burker-Turk chamber as size standard. Body volumes (v) were calculated using the equation, $v = 1/4\ ps^2/l$ (s = area of longitudinal section, l = length, average radius of worms = s/2l), by assuming that animals have a cylindrical shape.

Bioinformatics

The CEH-14 ChIP-seq data (Niu et al., 2011) were extracted, and the target gene list was used to retrieve gene information, expression information, and GO term information from WormMart (current data release WS220). The data was imported into Microsoft Excel™ and parsed according to cell and tissue types. GO terms were analyzed in GOrilla (Eden et al., 2009). For the multiple sequence alignment, genomic sequences were retrieved from WormBase (www.wormbase.org), aligned with SEAVIEW using the exons of *ceh-14* and *dpy-7* as anchors (Galtier et al., 1996), displayed in CLC Bio (www.clcbio.com), and further annotated. Putative binding sites for CEH-14 were searched for in JASPAR (Portales-Casamar et al., 2010) using the profile of the Drosophila ortholog LIM3 with a relative profile score threshold of 85%. Only predicted binding sites present both in *C. elegans* and *C. briggsae* are shown in Supplementary Fig. 1.

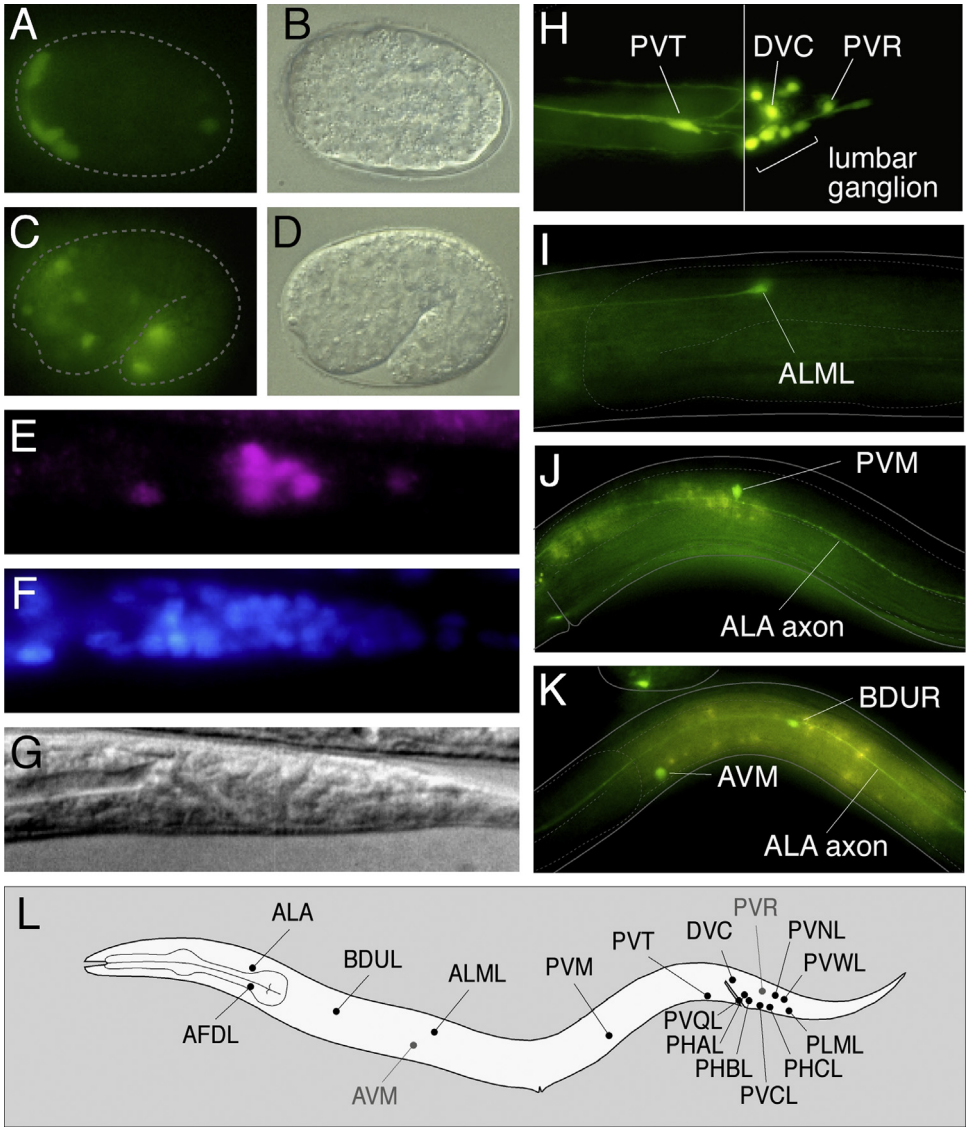

Fig. 2. Expression pattern of *ceh-14*. Embryos are oriented with anterior to the left, and hatched animals are oriented with anterior to the left and ventral to the bottom unless otherwise indicated. Fluorescent (A) and Nomarski (B) micrographs of GFP expression in a 280 min embryo, which carries the p4000E1::GFP reporter construct. The outline of the embryo is marked with white dashes. Fluorescent (C) and Nomarski (D) micrographs of GFP expression in comma stage embryo carrying p4000E1::GFP. (E)–(G) Micrographs of the tail region of a fixed wild-type worm, shown in Nomarski (G). The corresponding fluorescent images show CEH-14 as visualized using anti-CEH-14 immunostaining (E), and the nuclei stained with DAPI (F). (H) p4000E1::GFP expression in the tail region of a dorso-ventral aligned adult animal. The cell bodies of PVT, DVC, and PVR neurons are indicated. The other *ceh-14* expressing neurons in the (lumbar ganglion), PHA, PHB, PHC, PVC, PVN, PVQ and PVW, are shown in the bracket. (I)–(K) Integrated p4000E1::GFP expression in touch neurons. In (K), animal is oriented with anterior to the right to show AVM (right sided neuron). (L) Schematic representation of neuronal expression of *ceh-14*. Gray neurons (AVM and PVR) are located on the right side of the worm.

Results

Expression pattern of ceh-14 reporter constructs

To investigate the function of the LIM-HB gene *ceh-14*, we first analyzed the temporal and spatial expression pattern of *ceh-14* promoter reporter constructs (p4000E1::GFP) in transgenic worms (Figs. 1 and 2). *ceh-14* expression starts around the 280 min stage mainly in the anterior part of the embryo (Fig. 2A and B). In later stages (comma stage), the expression is seen in more cells in the head, but also in some cells in the tail (Fig. 2C and D). Judged by position and shape, most of them are neuronal precursors, although we have not precisely identified them. From larval to adult stages, neuronal expression is observed in the ALA interneuron and a pair of sensory neurons, AFDL/R, in the head, and in the BDUL/R interneurons in the anterior body (see also Cassata et al., 2000a). In the tail, we see expression in the sensory- and interneurons PHAL/R, PHBL/R, PHCL/R, DVC, PVCL/R, PVNL/R, PVQL/R, PVT, PVWL/R and PVR (Fig. 2H and L). The neuronal expression in the head and tail is confirmed by an anti-CEH-14 rabbit antiserum (Fig. 2E–G). We also note expression in the six touch neurons ALML/R, AVM, PVM and PLML/R (Fig. 2I–K), although it is seen only in strains with integrated reporter constructs. Detailed examination of the integrated reporter constructs shows that the expression of *ceh-14* in AFD is reduced in the *ceh-14*(*ch3*) mutant background compared to wild type or other neurons (see examples in Fig. 4B and C). This observation suggests that *ceh-14* is auto-regulated at least in the AFD neurons. GFP expression levels in the other neurons did not appear to be down-regulated. In addition to the neuronal expression, *ceh-14* expression is also seen in the hypodermis and spermatheca as previously described (Kagoshima et al., 2000).

Large scale ChIP-seq experiments conducted as part of modENCODE identified about 880 open reading frames, in the promoter

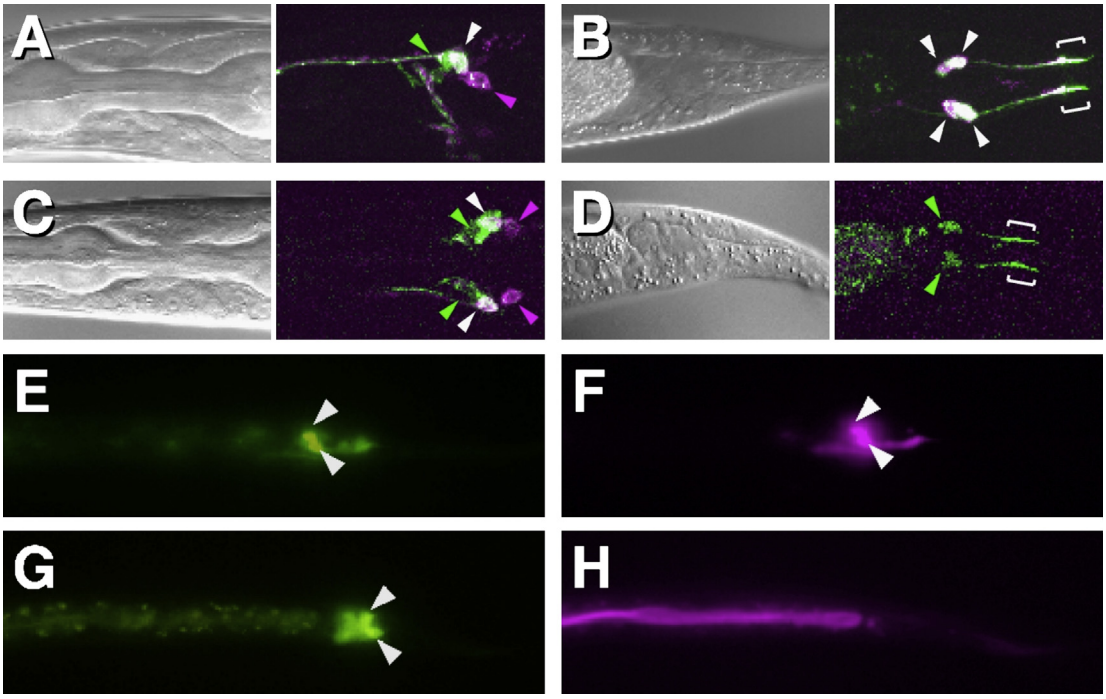

Fig. 3. Dye-filling defect in phasmid neurons in *ceh-14*(*ch3*) and its rescue by a functional *ceh-14::GFP construct.* (A)–(D) Nomarski and fluorescent micrograph of DiI stained animals carrying *gpa-13::GFP* (pRP2029) in wild type (A and B) and *ceh-14*(*ch3*) (C and D) backgrounds. Animals are mounted in lateral (A) or dorso-ventral (B–D) orientation. pRP2029 drives GFP expression in ADF, ASH, AWC, PHA and PHB. DiI strongly stains ASH, ASJ, ASK, ADL, PHA, and PHB in wild type. (A) Wild-type head. The colored arrowheads indicate the position of AWC (GFP: green), ASH (GFP and DiI: white) and ASJ (DiI: magenta). (B) Wild-type tail. The cell bodies and the ciliated endings of PHA and PHB are shown with white arrowheads and brackets, respectively. (C) *ceh-14*(*ch3*) head. The same DiI staining and GFP expression pattern are observed as in wild type. (D) *ceh-14*(*ch3*) tail. GFP expression is observed in the cell bodies (green arrowheads) and the ciliated endings (brackets) of a pair of PHA neurons, whereas DiI staining is absent in these neurons. PHB neurons are not visible in (D), because they are in the different focal plane. (E)–(H) Rescue of phasmid dye-filling defect by a functional *ceh-14::GFP* construct. (E) GFP expression in a *ceh-14*(*ch3*) mutant animal carrying p4000full::ΔNGFP (rescue construct). White arrows indicate the phasmid neurons, which express the functional fusion protein CEH-14::GFP. (F) Fluorescent micrograph of (E) showing DiI staining. Note that the phasmid neurons (white arrows) have regained their dye-filling ability. (G) GFP expression in a *ceh-14*(*ch3*) mutant animal carrying p4000E1::ΔNGFP (negative control). White arrows mark the phasmid neurons, which express the N-terminal 16 amino acids of CEH-14 fused to GFP. (H) Fluorescent micrograph of (G) showing lack of DiI staining (apart from gut ingestion).

region of which CEH-14 is potentially bound at the L2 stage (Niu et al., 2011). We examined this target gene list in order to determine, whether these genes are expressed in the cells we identified. We extracted annotation data for these genes (Supplementary Table I). Parsing of the data revealed 50 possible target genes that are expressed in the spermatheca, and 84 in the hypodermis, with 23 of them being expressed in both tissues. Neither visual inspection of these lists, nor analysis of the GO terms revealed any obvious enrichment. Possible target genes in the hypodermis linked to the cytoskeleton are *erm-1* (cytoskeletal linker), *tbb-2* (beta-tubulin), and *unc-115* (binds actin filaments). CEH-14 was shown to be a negative regulator of the collagen gene *col-43* in the spermatheca (Bando et al., 2005), though it is not present in this ChIP-seq list. About 180 genes have annotations relating to the nervous system, however, like quite a number of other genes, most of these are rather ubiquitously expressed. Only for a few genes were specific neuronal cell identifications made that allowed cross-referencing with the *ceh-14* expression pattern (Supplementary Table I). In AFD two interesting possible targets emerged, i.e. *ttx-7*, a myo-inositol monophosphatase member, and *pkc-1*(*ttx-4*), a protein kinase C member, both of which have been shown to play a role in thermosensation (Okochi et al., 2005; Tanizawa et al., 2006). An interesting putative target in the touch neurons is *mec-12*, an alpha-tubulin that is required for mechanosensory touch, specifically for the 15-protofilment microtubules in the touch cells (Fukushige et al., 1999). However, we did not observe a touch sensation defect in *ceh-14*(*ch3*) (Cassata et al., 2000a), and numerous genetic screens for touch sensation defects (Ernstrom and Chalfie, 2002; Syntichaki and Tavernarakis, 2004) did not yield any *ceh-14* mutations so far. Thus, while *ceh-14* may be involved in regulating *mec-12*, it could be redundant with other genes, for example, the LIM-HB gene *mec-3* that is required for touch neuron differentiation (Way and Chalfie, 1988).

Dissection of the ceh-14 promoter

We examined the expression pattern of promoter deletion derivatives to identify important regulatory regions for the *ceh-14* expression. The largest constructs p4000full::GFP and p4770E5::lacZ, containing promoter as well as large introns, show expression in all *ceh-14*-positive neurons (Fig. 2L), the spermatheca and the hypodermis. p4000E1::GFP, a promoter fusion construct, shows the same expression pattern as p4000full::GFP, except for a lack of hypodermal expression (Fig. 1). A deletion construct, p1650E1::GFP that removes the upstream 2.35 kb shows expression in AFD, BDU, PVQ and the spermatheca, but has lost expression in ALA, and most of the tail neurons and the touch neurons. The shorter p1240E1::GFP construct expresses in AFD, PVQ and the spermatheca, but BDU expression is lost. A minimal construct p240E1::GFP shows expression in the spermatheca and very faint expression in AFD, while p240E1::GFPlacZ shows weak expression only in the spermatheca (Fig. 1).

In conclusion, the regulatory region for the full expression is located in a region from 4 kb upstream to the fifth exon (regions A–E in Fig. 1). Region A, located from 4 kb to 1.65 kb upstream, is the important regulatory region for expression in ALA, the touch neurons and most of the tail neurons (DVC, PHA, PHB, PHC, PVC, PVN, PVT, PVW and PVR). The other elements for the expression map to region B for BDU, region C for AFD and PVQ, region D for the spermatheca, and to regions D and E, which encompasses the first introns, for the hypodermis (Fig. 1, Kagoshima et al., 2000).

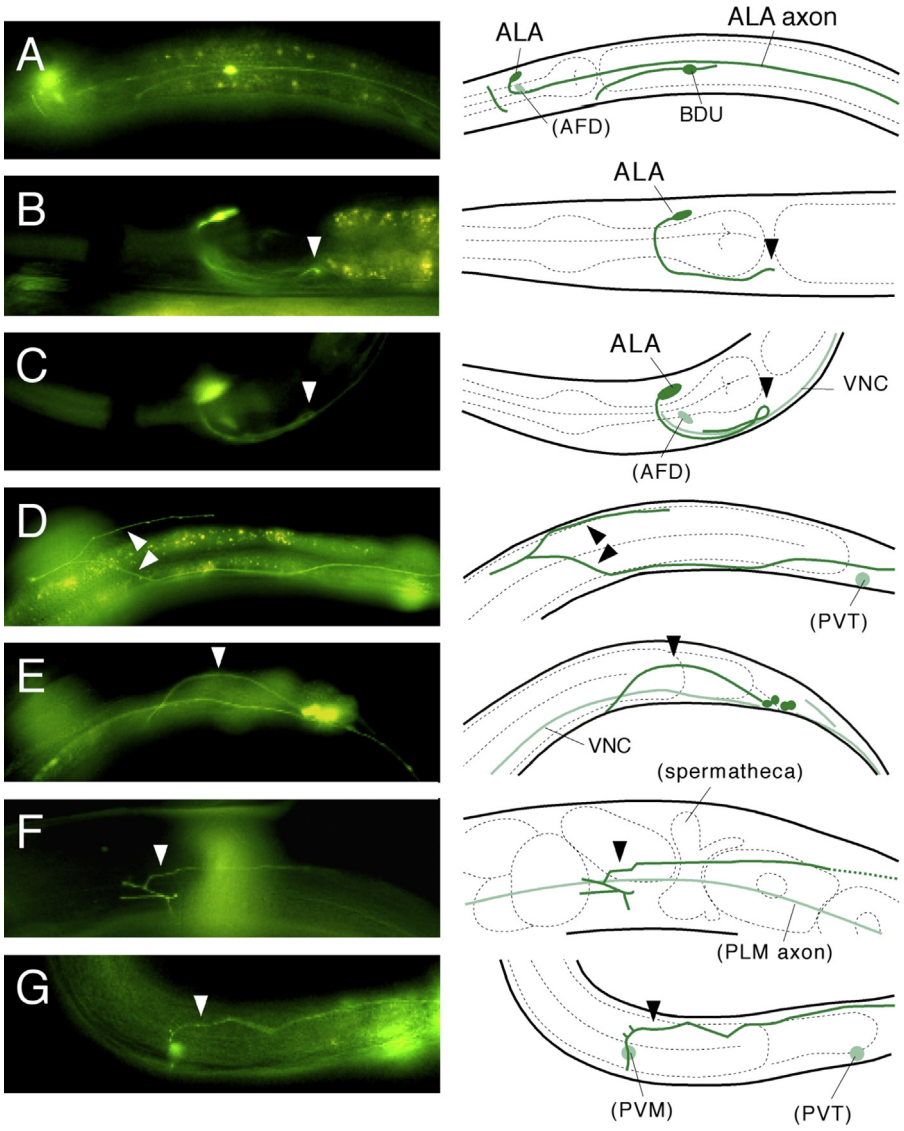

Fig. 4. Abnormal axonal morphologies in *ceh-14* mutants. Left panels show *ceh-14::GFP* expression (integrated p4000E1::ΔNGFP). Right panels are drawings showing the morphologies of the *ceh-14* expressing neurons. (A)–(C) Axonal morphology of the ALA neuron in different mutant backgrounds. (A) ALA axons in wild-type worms take lateral pathways. (B) The ALA axon runs into the VNC and stops immediately (arrow) in *ceh-14*(*ch3*). (C) ALA axons in *ceh-14*(*ch2*). Some worms show a phenotype, where ALA axons migrate "aimlessly". The abnormal loop structure of a selected ALA axon is indicated (triangle). Note the missing or reduced expression in AFD in (B) and (C). (D)–(G) Tail axon morphology in *ceh-14* mutant backgrounds. They show a variety of phenotypes, wandering, switching back and branching. (D) and (E) Abnormal tail axons in *ceh-14*(*ch3*) mutant backgrounds. (F) and (G) Abnormal tail axons in *ceh-14*(*ch2*) mutant backgrounds.

We compared the genomic sequences of *C. elegans*, *C. briggsae* and *C. remanei* over the regions A–E in order to identify conserved sequence elements. It revealed several regions with numerous conserved blocks (Supplementary Fig. 1). Three of these regions are in A (A1–A3), one in C (C1), and one in the first large intron (E1), and presumably contain the key elements for *ceh-14* regulation, e.g., E1 in intron 1 would be the prime candidate for driving expression in the hypodermis. Within the well conserved areas of A3 and E1 we note that recently two small non-coding RNAs (ncRNA) have been predicted by modENCODE (Gerstein et al., 2011), which are transcribed in the opposite direction of *ceh-14* (Fig.1, Supplementary Fig. 1). The CEH-14 ChIP-seq experiments have also identified three putative CEH-14 binding regions (in A1, A3, and C1) in the *ceh-14* promoter itself, indicative of autoregulation (Supplementary Fig. 1, Niu et al., 2011). The binding region in A3 overlaps with the ncRNA, while the one in C1 could be responsible for the autoregulation we observed in AFD. To detect putative, phylogenetically conserved CEH-14 binding sites in the sequence, we scanned the regulatory region with the binding profile of the fly ortholog LIM3 using JASPAR (Portales-Casamar et al., 2010). We identified near or within each region (A1, A3, and C1) three putative sites each (TAATTA consensus, Supplementary Fig. 1), and one in E1. Two of the sites in A3, and the one in E1 overlap with the ncRNAs. It is intriguing to speculate, whether the ncRNAs may be involved in regulating *ceh-14* by blocking transcription factor binding sites, while they are being transcribed.

Loss of a single LIM domain causes thermotaxis defects

We previously described two deletion mutant alleles: *ceh-14* (*ch1*), which deletes only intron sequences, and *ceh-14*(*ch3*), which is a loss of function deletion (Fig. 1, Cassata et al., 2000a). Here, we present one further allele, *ceh-14*(*ch2*). Genomic sequencing revealed that *ceh-14*(*ch2*) corresponds to a

Table 1
Isothermal tracking assays of *ceh-14*(*ch2*) mutant and rescued animals. The thermotaxis behavior is classified into five categories: (W), wild type response to thermal stimuli; (A), athermotactic response; (I), intermediate response between (W) and (A); (C), cryophilic response; (T), thermophilic response. p4000full::ΔNGFP is a rescue construct, carrying the full promoter and the entire ORF of *ceh-14*, and p4000E1::ΔNGFP is a negative control, carrying only the promoter region (Fig. 1). The number of animals examined are shown in column (N). The data marked by (*) were previously presented in Cassata et al. (2000a).

	Thermotaxis (%)					N
	W	I	A	C	T	
N2*	94	0	2	3	1	129
ceh-14(*ch2*)	50	18	17	3	12	103
ceh-14(*ch3*)*	33	22	40	2	3	108
ceh-14(*ch2*)+p4000E1::ΔNGFP	18	39	35	3	5	40
ceh-14(*ch2*)+p4000full::ΔNGFP	56	19	20	1	4	80
ceh-14(*ch3*)+p4000full::ΔNGFP*	63	18	10	6	3	114

Table 2
Phasmid dye-filling defect of *ceh-14* deletion mutants and their rescue by a functional *ceh-14::GFP* fusion construct. The animals were treated with DiI and examined for phasmid dye-filling. Only animals with amphid dye-filling (as internal control) were examined, the numbers examined are shown in column (N). Percentages of phasmid dye-filling are given for different mutant backgrounds in the absence or presence of transgenic arrays. The *ceh-14*(*ch2*) mutant allele and transgenic derivatives were examined in synchronized animals at late L2 to L3 larval stage.

	Phasmid dye filling (%)	N
N2	96.9	554
ceh-14(*ch1*)	97.0	367
ceh-14(*ch2*)	64.0	125
ceh-14(*ch2*)/+	84.3	64
ceh-14(*ch2*)+p4000E1::ΔNGFP	35.1	168
ceh-14(*ch2*)+p4000full::ΔNGFP	95.6	339
ceh-14(*ch3*)	1.3	318
ceh-14(*ch3*)/+	70.0	70
ceh-14(*ch3*)+p4000E1::ΔNGFP	8.7	103
ceh-14(*ch3*)+p4000full::ΔNGFP	84.7	255

deletion that extends from the second intron to the third intron, removing the third exon (Fig. 1). Since the second exon can splice in frame to the fourth exon, a transcript can be generated that encodes a protein lacking a major part of the first LIM domain. The presence of such a transcript was confirmed by sequencing RT-PCR products from *ceh-14*(*ch2*). Northern blot analysis shows a transcript of similar size and intensity to wild type, which is consistent with the notion that a stable message is generated (data not shown).

We have previously shown that the null mutation *ceh-14*(*ch3*) animals have severe defects in performing isothermal tracking (Table 1, Cassata et al., 2000a). *ceh-14*(*ch2*) animals display a mild, but clear athermotactic phenotype (Table 1). Rescue experiments of *ceh-14*(*ch2*) show a small restoration of thermotaxis by p4000full::ΔNGFP, which carries the entire coding sequence of *ceh-14*, although the difference is statistically not significant (Table 1). At the same time, we also observed an enhancement of the athermotactic phenotype in the case of p4000E1::ΔNGFP, which contains only a part of the first exon of *ceh-14* and was used as control. This effect could be caused by a titration of *ceh-14* regulating factors by multiple copies of the promoter sequence in the p4000E1::ΔNGFP array. We cannot unequivocally conclude that *ceh-14*(*ch2*) is rescued by p4000full::ΔNGFP from these results, however, it is consistent with the notion that *ceh-14*(*ch2*) is a loss-of-function mutation.

Phasmid dye-filling defects in ceh-14 mutants

The PHA and PHB pairs of neurons are the main sensory neurons in the phasmid sensilla located in the tail. They have ciliated endings at the tip of the dendrites that are open to the environment (White et al., 1986; Wood, 1988), and function as chemosensory cells that negatively modulate reversals to repellents (Hilliard et al., 2002). A simple test, dye-filling, can show if amphid and phasmid neurons are open towards the environment and are able to take up dye through their dendritic endings (Hedgecock et al., 1985; Ohkura and Bürglin, 2011; Perkins et al., 1986; Tong and Bürglin, 2010). The fluorescent dye DiI can stain strongly the sensory neurons ASH, ASJ, ASK, ADL (and weakly AWB, ASI) in the head, and PHA, PHB in the tail. We examined all three alleles of *ceh-14* for their dye-filling properties using DiI. *ceh-14*(*ch1*), with lacks only intron sequences and produces a wild-type transcript, has a wild-type percentage (97%) of dye-filling in phasmid neurons. In *ceh-14*(*ch2*), the animals are almost wild-type for dye-filling at the adult stage, whereas larvae show consistent defects (64%) at late L2 to L3. The null mutant *ceh-14*(*ch3*) shows almost no (1%) dye-filling (Table 2).

The Dyf phenotype of *ceh-14*(*ch3*) is rescued by a full-length construct p4000full::ΔNGFP (Fig. 3E and F, Table 2), while the negative control p4000E1::ΔNGFP is not able to rescue the defect (Fig. 3G and H, Table 2). We examined rescue with construct p4000full::ΔNGFP in synchronized *ceh-14*(*ch2*) worms at the late L2 to L3 stage. *ceh-14*(*ch2*) animals show dye-filling that can be rescued to 96% by p4000full::ΔNGFP. Control construct p4000E1::ΔNGFP has only 35% dye-filling, which is more severe than *ceh-14*(*ch2*) alone (Table 2). This enhanced phenotype is reminiscent of the thermotaxis phenotype observed with p4000E1::ΔNGFP in *ceh-14*(*ch2*). The *ceh-14*(*ch2*) allele may be a particularly sensitized mutant, as the severity of the mutant phenotype diminishes during development. To determine whether *ceh-14*(*ch2*) and *ceh-14*(*ch3*) are loss-of function alleles, we examined heterozygous worms containing the mutation over a wild-type allele. The results show that their dye-filling capacity is substantially restored compared to the homozygous mutants, reaching wild-type levels for *ceh-14*(*ch2*), and 70% for *ceh-14*(*ch3*) (Table 2). We thus propose that the two alleles are both loss-of-function mutants with respect to dye-filling.

The Dyf phenotype of *ceh-14* mutants is not due to the loss of phasmid neurons or failure in outgrowth of the dendrites. We investigated this by examining wild-type and *ceh-14*(*ch3*) animals carrying the *gpa-13::GFP* reporter, which visualizes the cell body and dendrites of ADF, AWC, and ASH in the head, and PHA, PHB in the tail (Fig. 3A D). *ceh-14*(*ch3*) animals show the same dye-filling pattern in the head as wild-type animals, whereas PHA and PHB fail to take up DiI in *ceh-14*(*ch3*). Although the phasmid dendrites are somewhat shorter than those of wild type, the length of the cilia structures appears normal in *ceh-14*(*ch3*) animals (Fig. 3D). Loss of dye-filling can be due to a number of defects that cause changes in cell morphology, i.e. loss of the sensory neuron, loss of dendrites, loss of the sensory cilia, or cilia that are not full length. This is not the case for *ceh-14*, where cell morphology and cilia length is wild-type, suggesting that the dye-filling defect may be caused by a failure of the phasmid endings to open to the environment. Alternatively, uptake or transport of the dye could be affected.

Since the dendrites are a bit shorter in *ceh-14* mutants than in wild type, and we had noted that *ceh-14* mutant animals seem generally smaller, we investigated the body size in *ceh-14*(*ch3*). The body length and volume of *ceh-14* mutants is similar to those of N2 until 48 h (from L1 to young adult stage), but *ceh-14* mutants are significantly smaller at 72 h after L1-arrest release (82% length, 56% volume, Supplementary Fig. 2). Judging from the gonadal morphology, the timing of larval development was indistinguishable between N2 and *ceh-14* mutants, indicating that body size

Table 3
ALA interneuron pathfinding defects in *ceh-14* deletion mutants. The ALA axons are visualized by a *ceh-14::GFP* construct, p4000E1::ΔNGFP, which is integrated in chromosome V. Genetic backgrounds are indicated in the first column. The percentage of animals in which both axons took the lateral path is given. Total number of worms examined are shown in the third column (N).

	ALA axons in lateral path (%)	N
Wild type	83.0	106
ceh-14(*ch2*)	11.9	101
ceh-14(*ch3*)	0.0	94

reduction in *ceh-14* mutants is not due to developmental retardation. Although *ceh-14* is expressed in the hypodermis, we have not formally proven that *ceh-14*(*ch3*) causes the phenotype. However, the shortening of the dendrites may simply be due to the general reduced body size of the *ceh-14*(*ch3*) strain.

The ChIP-seq data of Niu et al. (2011) revealed the transcription factor DAF-19 as a possible target of CEH-14 (Supplementary Table. I). *daf-19* encodes an RFX transcription factor that functions in all ciliated neurons, is required for the formation of the cilia, and mutants are Dyf (Swoboda et al., 2000). However, since *ceh-14* mutants have cilia in the phasmid and AFD neurons (Cassata et al., 2000a), the Dyf and thermotaxis phenotypes would be unlikely due to a downregulation of *daf-19*.

Axonal pathfinding abnormalities in ceh-14 mutant worms

The *ceh-14* expressing neuron ALA is a single cell situated in the dorsal ganglion just behind the nerve ring. Two major bilaterally symmetrical processes leave the cell body and run right and left around the nerve ring, leaving it laterally and running down the length of the animal (White et al., 1986). *ceh-14*(*ch3*) mutant worms have the ALA cell body at the normal position, however, in virtually all animals one or both axons do not run into the lateral cord, but into the ventral nerve cord (VNC) and stop just behind the posterior pharynx (Fig. 4A and B, Table 3). *ceh-14*(*ch2*) shows similar defects with less penetrance, but axons mostly continue to extend to the tail region (Table 3). Several worms had loop-shaped ALA axons at the point where they normally turn into the lateral cord or else in the VNC (Fig. 4C). We also observed high percentages of abnormal axons of the tail neurons, aberrant projection, extra-branching, and premature termination in *ceh-14*(*ch3*) (Fig. 4D and E) and *ceh-14*(*ch2*) mutants (Fig. 4F and G). In contrast, the axonal projections from the head neurons, AFD and BDU, seemed to be normal at least by the light and fluorescent microscopic observation of integrated p4000E1::ΔNGFP transgenic animals.

The paired-like homeobox gene *ceh-17* has been shown to be expressed in ALA and to affect outgrowth of its axons (Pujol et al., 2000). Examination of the expression of *ceh-14::GFP* (p4000E1::GFP) in *ceh-17*(*np1*) mutant animals showed that expression is still seen in ALA. Conversely, using antibody staining, we were able to detect CEH-17 expression in ALA in *ceh-14*(*ch3*), although the staining efficiency was not monitored (data not shown).

To test whether neuronal fates could be altered we ectopically expressed CEH-14 throughout the nervous system. Full-length *ceh-14* as well as the LIM domains only of *ceh-14* were separately fused to the pan-neuronal *rab-3* promoter and GFP. However, these strains showed high levels of embryonic and early larval lethality: p*rab-3*::*CEH-14::GFP*: 82% ($N=79$) arrested; p*rab-3*::*CEH-14-LIM-only::GFP*: 63% ($N=43$) arrested; prabGFPRim3′ control: 21% ($N=47$) arrested. Possibly the overexpression of CEH-14 or its LIM domains in the nervous system sequesters interacting factors such as LDB-1 (Cassata et al., 2000a), and in turn impairs the function of other LIM-HD factors.

Discussion

ceh-14 function in the nervous system

The neuronal expression of *ceh-14* starts around 280 min of embryonic development, which is the time for the developmental switch from generating neurons to starting axonal outgrowth (Sulston et al., 1983). The expression is maintained throughout the life time, from embryo to adult, suggesting that *ceh-14* is required for late functions of the neurons. *ceh-14* seems to be involved in two aspects of neuronal differentiation. One is to control expression of determinants that give specific terminal identities or characteristics to particular types of neurons, as seen in AFD and the phasmid sensory neurons. The other is neurite outgrowth, as seen in ALA and tail neurons.

The phasmid neurons have no major abnormality in axonal and dendritic outgrowth in *ceh-14* mutants, which suggests they are almost complete, but fail to adopt their terminal identity. In the case of AFD, *ceh-14* mutants cannot respond to temperature properly, but only the finger-like structures at the tip of the dendrites are enlarged, otherwise the morphology of the neurons is normal (Cassata et al., 2000a). *ceh-14* has been shown to be located towards the end of the regulatory cascade in AFD, where it is regulated by the paired-like homeobox gene *ttx-1* that plays a critical role for the identity of the AFD neurons (Satterlee et al., 2001).

Serendipitously we isolated a deletion *allele, ceh-14*(*ch2*), which lacks one LIM domain. Our analysis shows that this results most likely in a partial loss-of-function phenotype, in line with similar observations from flies (O'Keefe et al., 1998; Thor et al., 1999) and vertebrates (Cheah et al., 2000). The mutant phenotypes in AFD, PHA, and PHB are probably due to a lack of interaction with co-factor(s), such as LDB-1. We showed that point mutations in the LIM domains of CEH-14 abolish the interaction with *C. elegans* LDB-1 in yeast, and that *ldb-1* is expressed - amongst many other cells - in the phasmid sensory neurons (Cassata et al., 2000b). The *ceh-14*(*ch2*) allele has the special trait that the phasmid Dyf phenotype diminishes with age. This observation indicates that this is not a permanent developmental defect, but function can be restored even in late stages. A late or subtle role for *ceh-14* also exists in the DVC neuron, where *ceh-14* and *ceh-63* together regulate the transcription factor MBR-1, though no phenotypes have been observed so far (Feng et al., 2012).

ceh-14 plays an important role in the axonal outgrowth of ALA, since it is required for the initial pathfinding, and abnormal migration into the VNC is seen in mutants. By contrast, the paired-like homeobox genes *ceh-17* and *ceh-10* are involved in antero-posterior axonal growth of the ALA axons (Pujol et al., 2000; Van Buskirk and Sternberg, 2010). *ceh-14*, *ceh-17*, and *ceh-10* act in separate pathways, although *ceh-14* and *ceh-17* are linked via cross-regulation (Van Buskirk and Sternberg, 2010). The *ceh-14* analyses of Van Buskirk and Sternberg (2010) show some discrepancies with our data, however, most of this is probably explained by the use of different reporter constructs (see Supplementary Fig. 1) and methods, as well as the markers used to examine axonal outgrowth (*ceh-14*::GFP versus *unc-53*::GFP, which is downregulated in *ceh-14*(*ch3*)).

The outgrowth defects of *ceh-14* mutants in tail neurons have not been examined in detail yet. Only in PVT *ceh-14* has been shown to play a subtle role in axon guidance, where it is required for the regulation of several *zig* genes (Aurelio et al., 2003). In animals mutant in both the LIM-HB gene *lim-6* and *ceh-14* flip-over defects along the axonal paths in the VNC are observed. Furthermore, *ceh-14* was implicated to also in the flip-over process by regulating adhesion molecules in the PVQ neurons.

In conclusion, *ceh-14* plays many different roles that cannot be reduced to one common denominator, rather it is required for

diverse aspects of terminal neuronal differentiation. To unravel these functions, the full complement of target genes needs to be identified in each cell. The 880 putative targets from the modENCODE ChIP-seq data (Niu et al., 2011) represent a starting point that needs further verification, but there may still be scores of additional, unknown targets.

Note added in proof

Movies of spatio-temporal (4D) *ceh-14::GFP* expression during embryogenesis are available at http://www.endrov.net/paper/ceh14.

Acknowledgments

We would like to thank I. Mori and her group for critical advice in identification of neurons and performing thermotaxis assays. Further we thank C. Van Buskirk and P. Sternberg for sharing of unpublished information. We thank A. Fire for providing vectors and G. Jansen for the *gpa-13*::*GFP* reporter plasmid, Y. Andachi and Y. Kohara for providing the Tc1 insertion strain YK11, M. Koga for some strains and markers, M. Nonet for prabGFPim3′, and G. Aspöck, C. Dozier, J. Ewbank and Y. Ohsima for helpful advice and discussion. Nematode strains used in this work were provided by the *Caenorhabditis* Genetics Center, which is funded by the NIH National Center for Research Resources (NCRR). This work and H.K. was supported by the Novartis Foundation. H.K. was and is supported by a JSPS Postdoctoral Fellowship for Research Abroad, and Grant-in-Aid for Scientific Research (Kakenhi) (C) (No. 23510239) from JSPS. This work was supported by grants NF. 3100-040843.94 and NF. 31-50839.97 from the Swiss National Science Foundation and the Kanton Basel-Stadt. T.R.B. was supported by a START Fellowship (NF. 3130-038786.93) and grants from the Swedish Foundation for Strategic Research. We acknowledge the support of the Center of Biosciences and Södertörn University.

Appendix A. Supporting information

Supplementary data associated with this article can be found in the online version at http://dx.doi.org/10.1016/j.ydbio.2013.04.009.

References

Agulnick, A.D., Taira, M., Breen, J.J., Tanaka, T., Dawid, I.B., Westphal, H., 1996. Interactions of the LIM-domain-binding factor Ldb1 with LIM homeodomain proteins. Nature 384, 270–272.

Aurelio, O., Boulin, T., Hobert, O., 2003. Identification of spatial and temporal cues that regulate postembryonic expression of axon maintenance factors in the *C. elegans* ventral nerve cord. Development 130, 599–610.

Ausubel, F.M., Brent, R., Kingston, R.E., Moore, D.D., Seidman, J.G., Smith, J.A., Struhl, K., 1987. Current Protocols in Molecular Biology. Green Publishing Associates and Wiley-Interscience, New York.

Bando, T., Ikeda, T., Kagawa, H., 2005. The homeoproteins MAB-18 and CEH-14 insulate the dauer collagen gene col-43 from activation by the adjacent promoter of the Spermatheca gene sth-1 in Caenorhabditis elegans. J. Mol. Biol. 348, 101-112.

Bürglin, T.R., 2011. Homeodomain subtypes and functional diversity. Subcell. Biochem. 52, 95–122.

Cassata, G., Kagoshima, H., Andachi, Y., Kohara, Y., Dürrenberger, M.B., Hall, D.H., Bürglin, T.R., 2000a. The LIM homeobox gene *ceh-14* confers thermosensory function to the AFD neurons in *Caenorhabditis elegans*. Neuron 25, 587–597.

Cassata, G., Kagoshima, H., Prétôt, R.F., Aspöck, G., Niklaus, G., Bürglin, T.R., 1998. Rapid expression screening of *C. elegans* homeobox genes using a two-step polymerase chain reaction promoter-GFP reporter construction technique. Gene 212, 127–135.

Cassata, G., Röhrig, S., Kuhn, F., Hauri, H.P., Baumeister, R., Bürglin, T.R., 2000b. The *Caenorhabditis elegans* Ldb/NLI/Clim orthologue *ldb-1* is required for neuronal function. Dev. Biol. 226, 45–56.

Chalfie, M., Sulston, J., 1981. Developmental genetics of mechanosensory neurons of *Caenorhabditis elegans*. Dev. Biol. 82, 358–370.

Cheah, S.S., Kwan, K.M., Behringer, R.R., 2000. Requirement of LIM domains for LIM1 function in mouse head development. Genesis 27, 12–21.

Dawid, I.B., Breen, J.J., Toyama, R., 1998. LIM domains: multiple roles as adapters and functional modifiers in protein interactions. Trends Genet. 14, 156–162.

Eden, E., Navon, R., Steinfeld, I., Lipson, D., Yakhini, Z., 2009. GOrilla: a tool for discovery and visualization of enriched GO terms in ranked gene lists. BMC Bioinformatics 10, 48.

Epstein, H.F., Shakes, D.C., (Eds.), 1995. Caenorhabditis elegans: Modern biological analysis of an organism. *Methods in Cell Biology, Vol. 48*, Academic Press, Inc., San Diego, London.

Epstein, H.F., Shakes, D.C. (Eds.), 1995. Academic Press, Inc., San Diego, London.

Ernstrom, G.G., Chalfie, M., 2002. Genetics of sensory mechanotransduction. Annu. Rev. Genet. 36, 411–453.

Feng, H., Reece-Hoyes, J.S., Walhout, A.J., Hope, I.A., 2012. A regulatory cascade of three transcription factors in a single specific neuron, DVC, in *Caenorhabditis elegans*. Gene 494, 73–84.

Fire, A., 1992. Histochemical techniques for locating *Escherichia coli* beta-galactosidase activity in transgenic organisms. Genet. Anal. Tech. Appl. 9, 5–6.

Fire, A., Harrison, S.W., Dixon, D., 1990. A modular set of lacZ fusion vectors for studying gene expression in *Caenorhabditis elegans*. Gene 93, 189–198.

Freyd, G., Kim, S., Horvitz, R.H., 1990. Novel cysteine-rich motif and homeodomain in the product of the *Caenorhabditis elegans* cell lineage gene *lin-11*. Nature 344, 876–879.

Fukushige, T., Siddiqui, Z.K., Chou, M., Culotti, J.G., Gogonea, C.B., Siddiqui, S.S., Hamelin, M., 1999. MEC-12, an alpha-tubulin required for touch sensitivity in *C. elegans*. J. Cell Sci. 112, 395–403.

Galtier, N., Gouy, M., Gautier, C., 1996. SEAVIEW and PHYLO_WIN: two graphic tools for sequence alignment and molecular phylogeny. Comput. Appl. Biosci. 12, 543–548.

Gerstein, M.B., et al., 2011. Integrative analysis of the *Caenorhabditis elegans* genome by the modENCODE project. Science 330, 1775–1787.

Han, M., Sternberg, P.W., 1991. Analysis of dominant-negative mutations of the *Caenorhabditis elegans let-60 ras* gene. Genes Dev. 5, 2188–2198.

Hedgecock, E.M., Culotti, J.G., Thomson, J.N., Perkins, L.A., 1985. Axonal guidance mutants of *Caenorhabditis elegans* identified by filling sensory neurons with fluorescein dyes. Dev. Biol. 111, 158–170.

Hedgecock, E.M., Russell, R.L., 1975. Normal and mutant thermotaxis in the nematode *C. elegans*. Proc. Natl. Acad. Sci. USA 72, 4061–4065.

Hilliard, M.A., Bargmann, C.I., Bazzicalupo, P., 2002. *C. elegans* responds to chemical repellents by integrating sensory inputs from the head and the tail. Curr. Biol. 12, 730–734.

Hobert, O., D'Alberti, T., Liu, Y., Ruvkun, G., 1998. Control of neural development and function in a thermoregulatory network by the LIM homeobox gene *lin-11*. J. Neurosci. 18, 2084–2096.

Hobert, O., Mori, I., Yamashita, Y., Honda, H., Ohshima, Y., Liu, Y., Ruvkun, G., 1997. Regulation of interneuron function in the *C. elegans* thermoregulatory pathway by the *ttx-3* LIM homeobox gene. Neuron 19, 345–357.

Hobert, O., Tessmar, K., Ruvkun, G., 1999. The *Caenorhabditis elegans lim-6* LIM homeobox gene regulates neurite outgrowth and function of particular GABAergic neurons. Development 126, 1547–1562.

Hobert, O., Westphal, H., 2000. Functions of LIM-homeobox genes. Trends Genet. 16, 75–83.

Hope, I.A. (Ed.), Oxford University Press, New York. 1999. *C. elegans*. A Practical Approach..

Kadrmas, J.L., Beckerle, M.C., 2004. The LIM domain: from the cytoskeleton to the nucleus. Nat. Rev. Mol. Cell Biol. 5, 920–931.

Kagoshima, H., Sommer, R., Reinhart, B.J., Cassata, G., Ruvkun, G., Bürglin, T.R., 2000. Graded expression of *ceh-14* reporters in the hypodermis is induced by a gonadal signal. Dev. Genes Evol. 210, 564–569.

Kania, A., Johnson, R.L., Jessell, T.M., 2000. Coordinate roles for LIM homeobox genes in directing the dorsoventral trajectory of motor axons in the vertebrate limb. Cell 102, 161–173.

Karlsson, O., Thor, S., Norberg, T., Ohlsson, H., Edlund, T., 1990. Insulin gene enhancer binding protein Isl-1 is a member of a novel class of proteins containing both a homeo- and a Cys-His domain. Nature 344, 879–882.

Koch, B.J., Ryan, J.F., Baxevanis, A.D., 2012. The diversification of the LIM superclass at the base of the metazoa increased subcellular complexity and promoted multicellular specialization. PLoS One 7, e33261.

Landgraf, M., Roy, S., Prokop, A., VijayRaghavan, K., Bate, M., 1999. *even-skipped* determines the dorsal growth of motor axons in Drosophila. Neuron 22, 43–52.

Lundgren, S.E., Callahan, C.A., Thor, S., Thomas, J.B., 1995. Control of neuronal pathway selection by the *Drosophila* LIM homeodomain gene *apterous*. Development 121, 1769–1773.

Mello, C.C., Kramer, J.M., Stinchcomb, D., Ambros, V., 1991. Efficient gene transfer in *C. elegans*: extrachromosomal maintenance and integration of transforming sequences. EMBO J. 10, 3959–3970.

Mori, I., Ohshima, Y., 1995. Neural regulation of thermotaxis in *Caenorhabditis elegans*. Nature 376, 344–348.

Niu, W., et al., 2011. Diverse transcription factor binding features revealed by genome-wide ChIP-seq in *C. elegans*. Genome Res. 21, 245–254.

O'Keefe, D.D., Thor, S., Thomas, J.B., 1998. Function and specificity of LIM domains in *Drosophila* nervous system and wing development. Development 125, 3915–3923.

Ohkura, K., Bürglin, T.R., 2011. Dye-filling of the amphid sheath glia: Implications for the functional relationship between sensory neurons and glia in *Caenorhabditis elegans*. Biochem. Biophys. Res. Commun. 406, 188–193.

Okochi, Y., Kimura, K.D., Ohta, A., Mori, I., 2005. Diverse regulation of sensory signaling by *C. elegans* nPKC-epsilon/eta TTX-4. EMBO J. 24, 2127–2137.
Perkins, L.A., Hedgecock, E.M., Thomson, J.N., Culotti, J.G., 1986. Mutant sensory cilia in the nematode *C. elegans*. Dev. Biol. 117, 456–487.
Pfaff, S.L., Mendelsohn, M., Stewart, C.L., Edlund, T., Jessel, T.M., 1996. Requirement for LIM homeobox gene *Isl1* in motor neuron generation reveals a motor neuron-dependent step in interneuron differentiation. Cell 84, 309–320.
Portales-Casamar, E., et al., 2010. JASPAR 2010: the greatly expanded open-access database of transcription factor binding profiles. Nucleic Acids Res. 38, D105–D110.
Pujol, N., Torregrossa, P., Ewbank, J.J., Brunet, J.F., 2000. The homeodomain protein CePHOX2/CEH-17 controls antero-posterior axonal growth in *C. elegans*. Development 127, 3361–3371.
Sambrook, J., Russell, D.W. (Eds.), 2001. Molecular Cloning: A Laboratory Manual (3-Volume Set). Cold Spring Harbor Laboratory Press, Cold Spring Harbor, New York.
Sánchez-García, I., Osada, H., Forster, A., Rabbitts, T.H., 1993. The cysteine-rich LIM domains inhibit DNA binding by the associated homeodomain in Isl-1. EMBO J. 12, 4243–4250.
Satterlee, J.S., Sasakura, H., Kuhara, A., Berkeley, M., Mori, I., Sengupta, P., 2001. Specification of thermosensory neuron fate in *C. elegans* requires *ttx-1*, a homolog of otd/Otx. Neuron 31, 943–956.
Sharma, K., Leonard, A.E., Lettieri, K., Pfaff, S.L., 2000. Genetic and epigenetic mechanisms contribute to motor neuron pathfinding. Nature 406, 515–519.
Sharma, K., Sheng, H.Z., Lettieri, K., Li, H., Karavanov, A., Potter, S., Westphal, H., Pfaff, S.L., 1998. LIM homeodomain factors Lhx3 and Lhx4 assign subtype identities for motor neurons. Cell 95, 817–828.
Srivastava, M., Larroux, C., Lu, D.R., Mohanty, K., Chapman, J., Degnan, B.M., Rokhsar, D.S., 2010. Early evolution of the LIM homeobox gene family. BMC Biol. 8, 4.
Sulston, J.E., Schierenberg, E., White, J.G., Thomson, J.N., 1983. The embryonic cell lineage of the nematode *Caenorhabditis elegans*. Dev. Biol. 100, 64–119.
Swoboda, P., Adler, H.T., Thomas, J.H., 2000. The RFX-type transcription factor DAF-19 regulates sensory neuron cilium formation in *C. elegans*. Mol. Cell 5, 411–421.
Syntichaki, P., Tavernarakis, N., 2004. Genetic models of mechanotransduction: the nematode *Caenorhabditis elegans*. Physiol. Rev. 84, 1097–1153.
Tanizawa, Y., Kuhara, A., Inada, H., Kodama, E., Mizuno, T., Mori, I., 2006. Inositol monophosphatase regulates localization of synaptic components and behavior in the mature nervous system of *C. elegans*. Genes Dev. 20, 3296–3310.
Thaler, J., Harrison, K., Sharma, K., Lettieri, K., Kehrl, J., Pfaff, S.L., 1999. Active suppression of interneuron programs within developing motor neurons revealed by analysis of homeodomain factor HB9. Neuron 23, 675–687.
Thaler, J.P., Koo, S.J., Kania, A., Lettieri, K., Andrews, S., Cox, C., Jessell, T.M., Pfaff, S.L., 2004. A postmitotic role for Isl-class LIM homeodomain proteins in the assignment of visceral spinal motor neuron identity. Neuron 41, 337–350.
Thor, S., Andersson, S.G., Tomlinson, A., Thomas, J.B., 1999. A LIM-homeodomain combinatorial code for motor-neuron pathway selection. Nature 397, 76–80.
Tong, Y.G., Bürglin, T.R., 2010. Conditions for dye-filling of sensory neurons in *Caenorhabditis elegans*. J. Neurosci. Methods 188, 58–61.
Van Buskirk, C., Sternberg, P.W., 2010. Paired and LIM class homeodomain proteins coordinate differentiation of the *C. elegans* ALA neuron. Development 137, 2065–2074.
Way, J.C., Chalfie, M., 1988. *mec-3*, a homeobox-containing gene that specifies differentiation of the touch receptor neurons in *C. elegans*. Cell 54, 5–16.
White, J.G., Southgate, E., Thomson, J.N., Brenner, S., 1986. The structure of the nervous system of the nematode *Caenorhabditis elegans.* Phil. Trans. R. Soc. Lond. B. 314, 1–340.
Wood, W.B., 1988. The Nematode *Caenorhabditis elegans*. Cold Spring Harbor Laboratory Press, Cold Spring Harbor, New York.
Zheng, Q., Zhao, Y., 2007. The diverse biofunctions of LIM domain proteins: determined by subcellular localization and protein-protein interaction. Biol. Cell 99, 489–502.